

# Effect of difference in shear modulus of phantom on displacement distribution induced by acoustic radiation force of focused ultrasound

## 集束超音波の音響放射圧によって生じたファントムの変位分布に対する剛性率の影響

Erika Numahata<sup>1†</sup>, Shin-ichiro Umemura<sup>1</sup>, and Shin Yoshizawa<sup>2,3</sup>

(<sup>1</sup>Grad. School of Biomed. Eng., Tohoku Univ.; <sup>2</sup>Grad. School of Eng., Tohoku Univ.;

<sup>3</sup>SONIRE Therapeutics)

沼畑瑛里香<sup>1†</sup>, 梅村晋一郎<sup>1</sup>, 吉澤晋<sup>2,3</sup>

(<sup>1</sup>東北大院 医工, <sup>2</sup>東北大院 工, <sup>3</sup>ソニア・セラピューティクス)

### 1. Introduction

High-intensity focused ultrasound (HIFU) treatment is one of the noninvasive treatments for cancer. In this treatment, the tumor is thermally coagulated by focusing ultrasound generated outside the body onto the target. With this method, the treatment region cannot be directly observed by optical method. Therefore, the prediction of the HIFU treatment region in advance by ultrasound imaging is important for the efficacy and safety of the treatment.

The previous study<sup>1)</sup>, showed that acoustic radiation force (ARF) imaging is a useful indicator of heat generated in the HIFU focal region. This estimation method is based on the approximation that the distribution of HIFU heat source is proportional to that of the ARF induced by a HIFU short burst. Since ARF induces a tissue displacement, the displacement distribution is proportional to the ARF distribution, when neglecting the effect of shear wave propagation. Therefore, the distribution of HIFU heat source was estimated from the ultrasonic measurement of the tissue displacement distribution.

However, this method still has some issues in quantitativity. In this study, tissue mimicking phantoms with different shear moduli were used to evaluate the effect of shear modulus on the estimation of the radiation force distribution.

### 2. Materials and Methods

#### 2.1. HIFU heat source estimation

When a tissue is exposed to ultrasonic waves, ARF is generated. ARF  $F$  and the acoustic intensity  $I$  are proportional.

On the other hand, the heat  $Q$  generated by HIFU exposure can be approximated to be

proportional to the acoustic intensity. Assuming that the acoustic attenuation is proportional to the absorption, the displacement induced by  $F$  can be regarded as proportional to  $Q$ .

The shear wave propagation velocity  $c_s$  when a shear wave propagates is expressed as,

$$c_s = \sqrt{G/\rho}, \quad (1)$$

where  $G$  is the shear modulus of elasticity (stiffness modulus) and  $\rho$  is the density. Therefore, the stiffness modulus is proportional to the square of the shear wave propagation velocity.

In summary, assuming that the displacement induced by ARF is caused only by shear deformation, the displacement is inversely proportional to the stiffness modulus and square of the shear wave propagation velocity.

#### 2.2. Experimental setup and Sequence

The experimental setup is shown in **Fig. 1**. A push beam for ARF was generated by a 128-channel linear probe (Hitachi Aloka Medical) connected to an ultrasound imaging system (Verasonics, Vantage 256), driving the central 20 elements and setting the focus at a depth of 16 mm from the surface of the phantoms (OST ELPT-018). The phantoms have shear wave velocities of 1.15, 1.6, and 3.2 m/s. By using the same linear probe and imaging system, RF data is acquired.

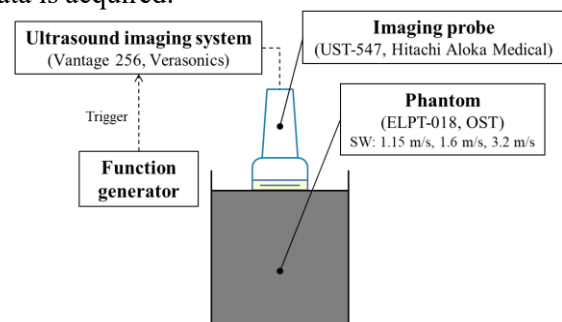


Fig. 1 Schematic of experimental setup.

**Fig. 2** shows the ultrasound exposure sequence for push beam transmission and RF data acquisition. A push beam at a voltage of 50 V and a duration of 90  $\mu\text{s}$  at a frequency of 6 MHz was focused to the phantom, and a single plane wave at 7.5 MHz was transmitted from the imaging probe before and after the push beam exposure. The axial displacement is calculated by applying the 2D combined autocorrelation method<sup>2)</sup> between the frames before and after the push beam exposure. It was measured that it took 416-418  $\mu\text{s}$  to transmit an imaging pulse after the end of the push beam exposure in this experiment.

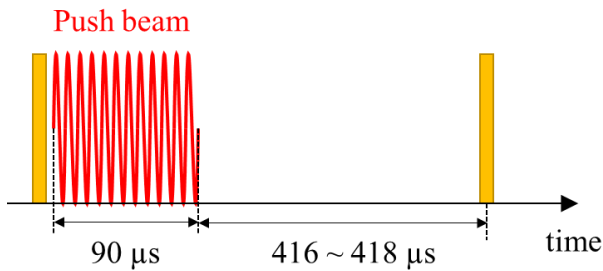


Fig. 2 Ultrasound exposure sequence.

### 3. Results and Discussion

**Fig. 3** shows the displacement distributions in the three phantoms with different shear wave propagation velocities, about 400  $\mu\text{s}$  after the end of the push beam. In all phantoms, the displacement in the shallower area than the focal point at a depth of 16 mm took the maximum value. Since the location of the maximum displacement shifts toward the shallower region as the shear wave propagation proceeds<sup>3)</sup>, so the larger the shear modulus is, the shallower the location of the maximum displacement should be. In Fig. 3, the phantom with a shear wave propagation velocity of 3.2 m/s, which has the highest shear modulus among the three, shows the maximum displacement about 10 mm in front of the focal point.

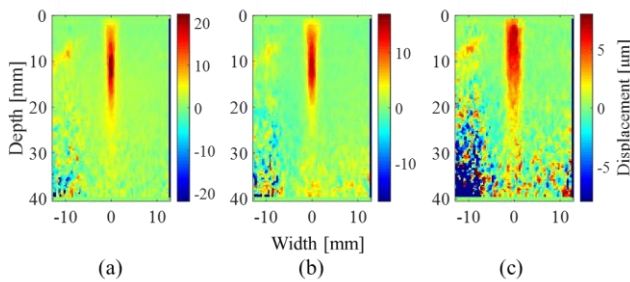


Fig. 3 Displacement distributions in the three phantoms with shear wave velocities of (a) 1.15 m/s, (b) 1.6 m/s, and (c) 3.2 m/s.

**Fig. 4** shows the averaged values of the measured displacements over the ROI (from 9.0 to 11.0 mm and -1.0 to 1.0 mm in axial and lateral directions, respectively) in each phantom. The average displacements in the phantoms with shear wave propagation speeds of 1.15, 1.6, and 3.2 m/s were  $13.1 \pm 0.8$ ,  $10.6 \pm 0.2$ , and  $5.4 \pm 0.4$   $\mu\text{m}$ , respectively. Comparing these values, it is seen that the ratio of the average displacement was close to the inverse ratio of the shear wave propagation velocity, rather than that of the shear modulus. The half-widths of the displacement distribution in the phantoms with shear wave propagation speeds of 1.15, 1.6, and 3.2 m/s were 1.4, 1.4, and 2.9 mm, respectively.

The effect of the shear wave propagation was clearly shown in the result of the half-width in the 3.2 m/s phantom. The shear wave propagation may have caused the larger average displacement in the 3.2 m/s phantom than that in the 1.6 m/s phantom divided by the ratio of shear modulus. The measurement of the acoustic absorption coefficients will be also needed to compare the displacements in detail.

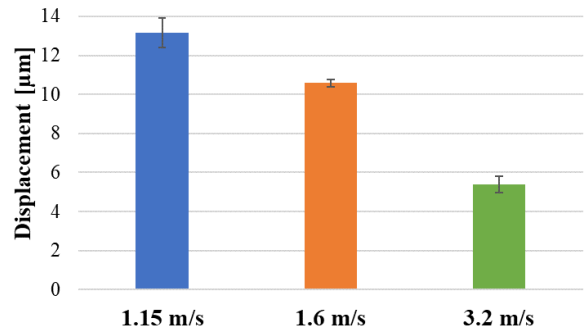


Fig. 4 Average displacements in ROI in the three phantoms with different shear modulus.

### 4. Conclusion

In this study, the quantitative performance of ARF imaging was evaluated by measuring the displacement in phantoms with different shear modulus for the quantitative estimation of HIFU heat source distribution. While a negative correlation between the displacement and shear modulus was observed, further study is needed for the detail analysis to consider the effect of shear wave propagation.

### References

1. H. Yabata, et al.: Jpn. J. Appl. Phys. 60, (2021) SDDE23
2. T. Shiina, et al.: J. Med. Ultrason. 29, (2002) 119.
3. M. L. Palmeri et al.: IEEE Trans. Ultrason. Ferroelect. Freq. Contr. 52, (2005) 1699.